

**Hydrated alumina as a calibrant for analysis of dust particle samples by single particle infrared spectroscopy**

A Senior Honors Thesis

Presented in Partial Fulfillment of the Requirements of the *graduation with research distinction in Chemistry* in the undergraduate college of the Ohio State University.

By

Charles Loney

Undergraduate Honors Thesis Program in Chemical Engineering

The Ohio State University

2016

James Coe (PhD), Advisor

Honors Thesis Committee: Professor James V. Coe, Professor Jeffrey Chalmers

Project Advisor: Professor James V. Coe, Department of Chemistry

Copyright by  
Charles Loney  
2016

## **Abstract**

Single particle Fourier transform infrared (FTIR) spectroscopy provides the volume fractions of chemical constituents in particulate matter by means of a Mie-Bruggeman model developed by our research group. Other techniques, such as electron microscopy, x-ray methods, and mass spectrometry, provide elemental analysis, and it is known that there is aluminum in many dust samples. We are interested in using single particle infrared spectroscopy to quantify and identify the aluminum containing compounds rather than just the elemental aluminum. The Mie-Bruggeman model currently includes quartz, calcite, dolomite, three types of clay, gypsum, and three types of organic molecules. This work describes the addition of hydrated alumina to the model. The next part of the project will involve applying this model to single particle spectral libraries of dust from our lab air, a house-filter, snow piles from High Street, the 9/11/01 World Trade Center event, and the International Space Station. Identifying the specific composition in such dust samples will yield benefits ranging from scientific understanding to being capable of discerning new health risks.

## **Vita**

2008 – 2012.....Fairview High School

Fairview Park, OH

2012 to present..... B.S. Chemical Engineering, Department of Engineering

The Ohio State University

## **Fields of Study**

Major Field: Chemical Engineering

## **Acknowledgments**

I would like to thank Dr. Coe and all the group members for all of the knowledge and support they have shared with me throughout our experiences together.

## Table of Contents

Abstract .....	3
Vita.....	4
Acknowledgements.....	5
List of Figures/Tables .....	7
Chapter 1: Introduction .....	8
Chapter 2: Plasmonic Nature of Mesh .....	11
Chapter 3: Methodology .....	13
Chapter 4: Results and Discussion (Mie Theory) .....	17
Chapter 5: Results and Discussion (Mie-Bruggeman Theory) .....	20
Chapter 6: Future Work and Conclusions.....	26
Bibliography .....	27
Appendix A: Individual Hydrated Alumina Spectra Sorted by Bottle .....	28

## List of Figures/Tables

<b>Figure 1.1:</b> Aluminum concentrations in various environment samples <sup>1</sup> .....	9
<b>Figure 1.2:</b> Using single-particle mass spectrometry to discern data for aluminum particles collected during the ACE-Asia field campaign <sup>12</sup> . ....	10
<b>Figure 2.1:</b> IR spectra of single 5 $\mu\text{m}$ diameter latex spheres on a ZnSe window (top) and within a hole of metal micromesh (bottom). Dominant scattering effects are diminished by plasmonic mesh.....	12
<b>Figure 3.1:</b> A reflectance image of a hydrated alumina sample (from a bottle labeled “gibbsite”). .....	14
<b>Figure 3.2:</b> A 2D contour image of 2 gibbsite particles before Chemimap is used. ....	15
<b>Figure 3.3:</b> A 2D contour image of 2 gibbsite particles after Chemimap is used. It is clearly much more obvious that there are two particles in this region, as opposed to the information illustrated from Figure 3.2. ....	16
<b>Figure 4.1:</b> Nine hydrated alumina spectra, soon to be average for Figure 6. ....	17
<b>Figure 4.2:</b> -OH stretch of pinosresinol using infrared ion-gain spectroscopy (no significant hydrogen bonding) <sup>13</sup> .....	18
<b>Figure 4.3:</b> Average of 9 particle spectra of hydrated alumina .....	19
<b>Figure 5.1:</b> The average fit from Figures A1-A7 graphed with the experimental fit from Mie Theory. ...	20
<b>Table 1:</b> Hydrated Alumina Mie Fit Parameters of the Average of 18 Particle Spectra; the Fitted Radium is 2.178 $\mu\text{m}$ and $\epsilon_0 = 1.75$ .....	21
<b>Figure 5.2:</b> Flow diagram for a visual representation of Mie-Bruggeman theory <sup>2</sup> . ....	23
<b>Figure 5.3:</b> Mie-Bruggeman model fits. Mixture model fits of the average IR spectra from single particle collections of lab air, house dust from a filter, and the WTC 9/11/2001 event <sup>6</sup> . ....	24
<b>Figure 5.4:</b> Volume fractions for given calibrants, which are iteratively calculated from the Bruggeman theory from the equation presented in Figure 8 <sup>6</sup> .....	24
<b>Figure A1:</b> Individual hydrated alumina particles from bottle labeled “alumina.” .....	29
<b>Figure A2:</b> Individual hydrated alumina particles from bottle labeled “gibbsite.” .....	29

## Chapter 1: Introduction

The chemical composition of many particulate matter sample fragments is unknown. The focus of this study is to add calibrants (pure materials) thought to be in the dust of interest into the infrared dust model and, ultimately, to use such infrared models to yield insight on the component fractions of dust samples. Certain imaging techniques – such as electron microscopy, x-ray methods, and mass spectrometry – can all be used for analysis on dust particles. These methods, however, can take a long time, can destroy the particle during the operation, and, most crucially, only provide elemental analysis.

Fine particles are generally considered more important than coarse ones in air monitoring with regards to public health because the former penetrate and are retained more deeply in the human respiratory tract<sup>1</sup>. Therefore, in one study, the concentration of soil-driven particles in atmospheric aerosol samples is found using methods presented by the National Air Surveillance Network (NASN) of Japan<sup>1</sup>. Excess added aluminum in airborne particulate matter (APM) (<10  $\mu\text{m}$ ) is also determined because aluminum is so widely used in industry and daily activity. Therefore, even though the source of aluminum in the atmosphere is mainly wind-blown soil particles, human activities such as metal industry, fuel combustion, and so on, can be origins of excess Al in the atmosphere. This is depicted in Figure 1:



Sample	Al (mg g <sup>-1</sup> )
Fuel-oil combustion	10
Cement	65
Refuse incineration	11
Iron and steel industry	10
Asphalt pavement	71
Gasoline automobile	1.5
Shale	80
Kosa, yellow sand	67
Coal	31
Crust	82.3
Japanese soil*	90.3
Coal fly ash	140
Marine aerosol	$0.3 \times 10^{-3}$

**Figure 1.1:** Aluminum concentrations in various environment samples<sup>1</sup>.

This information illustrates that Al is a necessary indicator element for the characterization of the atmospheric aerosol. What is currently unknown, however, is the specific composition of Al compounds in these samples. The goal of this research is to discern this composition as well as its amount. To further illustrate this point, consider Figure 1.2:

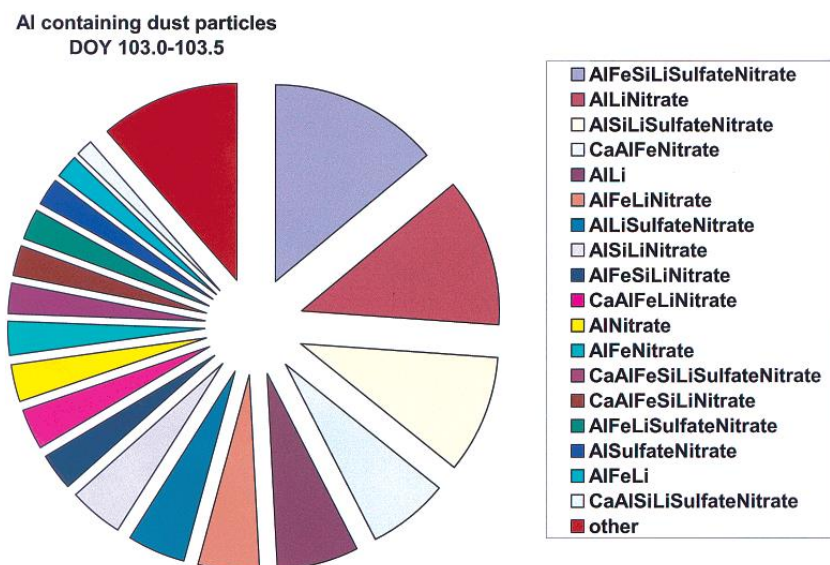


**Figure 1.2:** Using single-particle mass spectrometry to discern data for aluminum particles collected during the ACE-Asia field campaign<sup>12</sup>. In this figure, the particles are classified and sorted according to different types. The data shown in the pie graph represent the complexity of mineral dust particles containing aluminum in the troposphere.

There are also some established safety protocols regarding APM. The EPA sets a 24-hour standard of  $35 \mu\text{g}/\text{m}^3$  for particulate matter (PM) smaller than  $2.5 \mu\text{m}$  and  $150 \mu\text{g}/\text{m}^3$  for PM smaller than  $10 \mu\text{m}$ . More information regarding particle composition in the size range between  $2.5$  and  $10 \mu\text{m}$  would be particularly useful since these particles get inside of human lungs. Furthermore, because the airborne lifetime of particles decreases as the particle diameter increases, particles of  $\sim 4 \mu\text{m}$  in diameter are expected to be more correlated with the local environment, and thus health. Substances such as elemental carbon, calcium, vanadium, and organic carbon material in PM have illustrated strong positive correlation with respiratory health effects<sup>2</sup>. An extreme illustration of disease caused by particulate matter is the “London Smog” of Dec. 4—9, 1952, in which approximately 300 times the normal amount ( $7000 \mu\text{g}/\text{m}^3$ ) of PM is thought to have killed 12,000 people<sup>2</sup>.

## Chapter 2: Plasmonic Nature of Mesh

The main novel idea with this project is that it utilizes the phenomenon of plasmonics (interaction of IR light and conducting metal electrons) to trap light in holes that are smaller than the wavelength of that light itself. To achieve this, a gold mesh containing square holes  $5\text{ }\mu\text{m}$  that is spaced by  $12.7\text{ }\mu\text{m}$  is cut and attached to a washer about the size of a quarter. It has been previously demonstrated that IR transmission modes mediated by surface plasmon polaritons run rampant across the surface of a plasmonic mesh<sup>2</sup>. As a result, a particle in a subwavelength mesh hole experiences radiation very differently than an isolated particles: light incident on an isolated, wavelength-scale particle is dominated by scattering, which is well-modelled by Mie theory. On the other hand, a particle in a mesh hole is touched on four sides by surfaces carrying evanescent waves. The mesh spectra are dominated by absorption and are free of the usual Mie scattering effects. To illustrate this phenomenon, spectra of twenty individual  $5\text{ }\mu\text{m}$  diameter latex (polystyrene) spheres were averaged as shown in the top of Figure 2, while nineteen single spectra of mesh holes were averaged to obtain the spectrum in the bottom panel of Figure 2.1<sup>2</sup>.

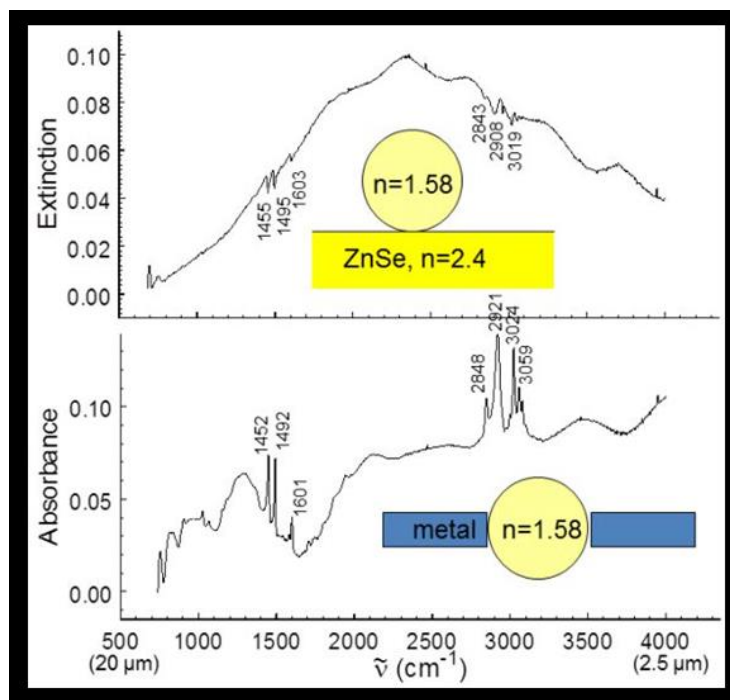


**Figure 2.1:** IR spectra of single 5  $\mu\text{m}$  diameter latex spheres on a ZnSe window (top) and within a hole of metal micromesh (bottom). Dominant scattering effects are diminished by plasmonic mesh.

Spectra of hydrated alumina are presented in Appendix A using methods similar to the ones used when recording the IR spectra of latex spheres. It is worth noting that the most common type of alumina is  $\gamma$ -alumina ( $\gamma\text{-Al}_2\text{O}_3$ ), and the two most common types of alumina hydroxide are gibbsite ( $\alpha\text{-Al}(\text{OH})_3$ ) and bayerite ( $\beta\text{-Al}(\text{OH})_3$ )<sup>10</sup>. However, none of the particles from the bottles labeled “gibbsite” are actually gibbsite, and much of the alumina is hydrated (discussed in more detail in Chapter 4).

### Chapter 3: Methodology

The calibrant, or unknown compound thought to be in the dust samples of interest, is added to the gold mesh. This calibrant (hydrated alumina), is in the form of powder. A vacuum is run (~1 min) to trap the particles in the actual mesh holes. Next, a Perkin-Elmer Spotlight 300 IR microscope is used in combination with an FTIR to acquire a full spectra at each 6.25  $\mu\text{m}$  square pixel within the imaging region. By using both reflection and transmission optical modes, it can be discerned that the particles is contained in the hole, but little else<sup>3</sup>. To begin this process, a region of interest is found and marked. The imaging spectra are recorded at 4  $\text{cm}^{-1}$  resolution using 512 scans per pixel<sup>4</sup>. The range is 700-4,000  $\text{cm}^{-1}$ , and the imaging mode is transmission. A background is also taken on a region of empty mesh holes.

In the example shown below in Figure 3.1, a square region of ~65  $\mu\text{m}$  is drawn over 2 particles of interest (note: a third particle appears to be in the square window; however, it is not actually trapped in a hole and therefore is not enhanced).

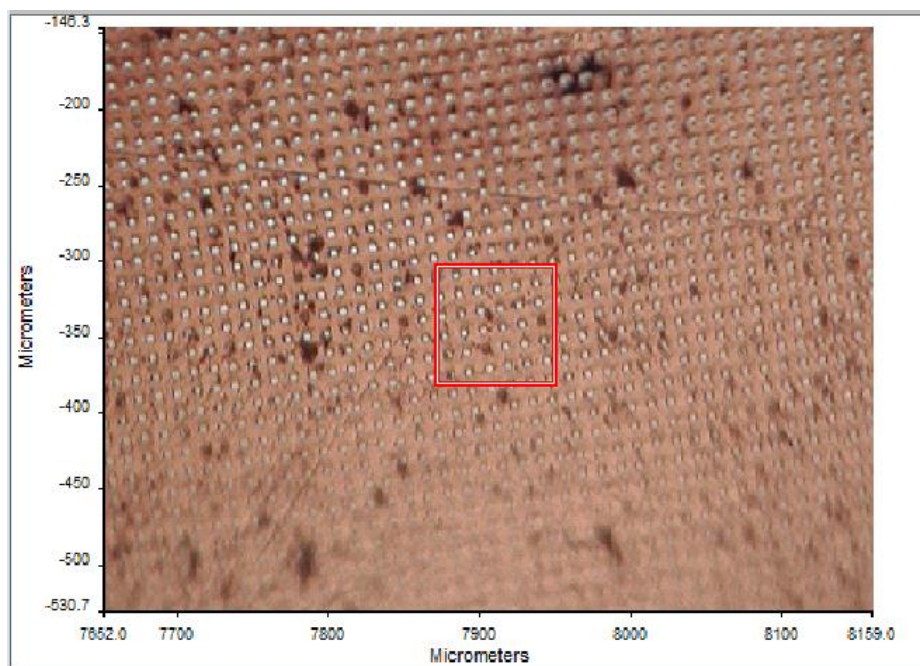


**Figure 3.1:** A reflectance image of a hydrated alumina sample (from a bottle labeled “gibbsite”).

Next, each spectrum found is specified for analysis by employing “ballpark” estimates of where particle signatures might lie (a software tool in the Perkin-Elmer program called Chemimap does this). In other words, within the raw spectra given by the 2D contour plot, the user picks wavenumbers of material of interest such that the contour shows high density absorbance values. This analysis is to better identify where particles might hide and, likewise, to better hide where background is otherwise sensitive and misleading. For example, in Figure 3.2 shown below, the contour plot clearly illustrates one particle, located toward the bottom-right portion of the graph. However, there is another, not-so-obvious particle to the bottom left that is more explicitly identified through using the Chemimap tool to increase the sensitivity of particles with spectra shown by the obvious particle given. Similarly, if this “greenish” particle is not actually relevant to the study, it will blend in with the background. In this case, it is indeed a particle (Figure 3.3). For comparison, the reflectance image corresponding to the 2D window is shown on the right of Figure 3.2.

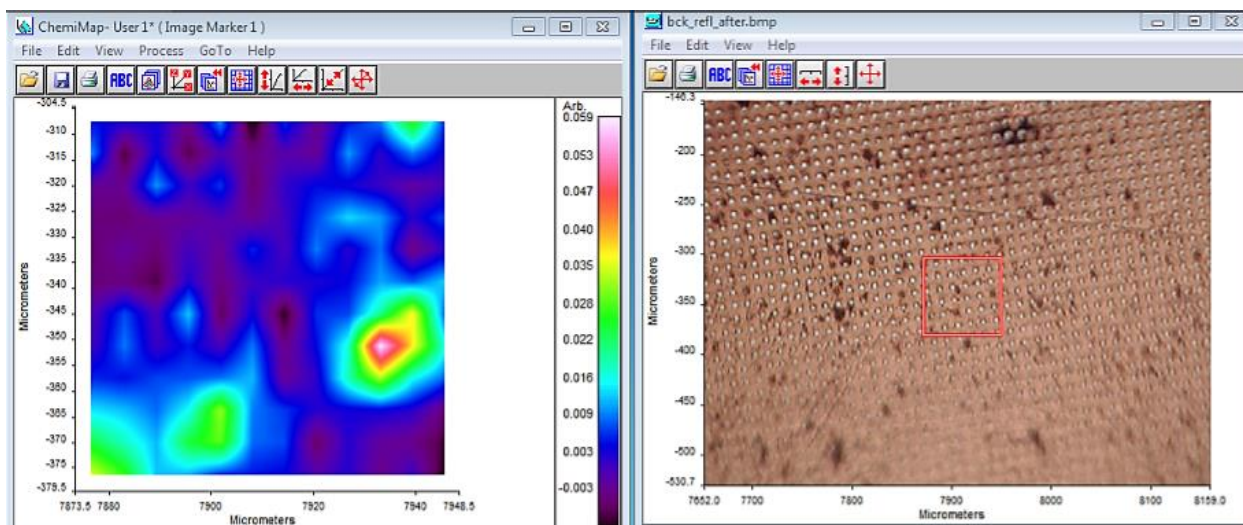


**Figure 3.2:** A 2D contour image of 2 gibbsite particles before Chemimap is used.

For hydrated alumina, a Chemimap setting of 2,700 and 3,700 wavenumbers are used for the Base 1 and Base 2 settings, respectively, with the “Start” at 3,300 wavenumbers. For each analyzed spectrum, two windows of 3 pixels by 3 pixels long are chosen in Chemimap: one containing the particle of interest, and the other containing an empty hole for a background.

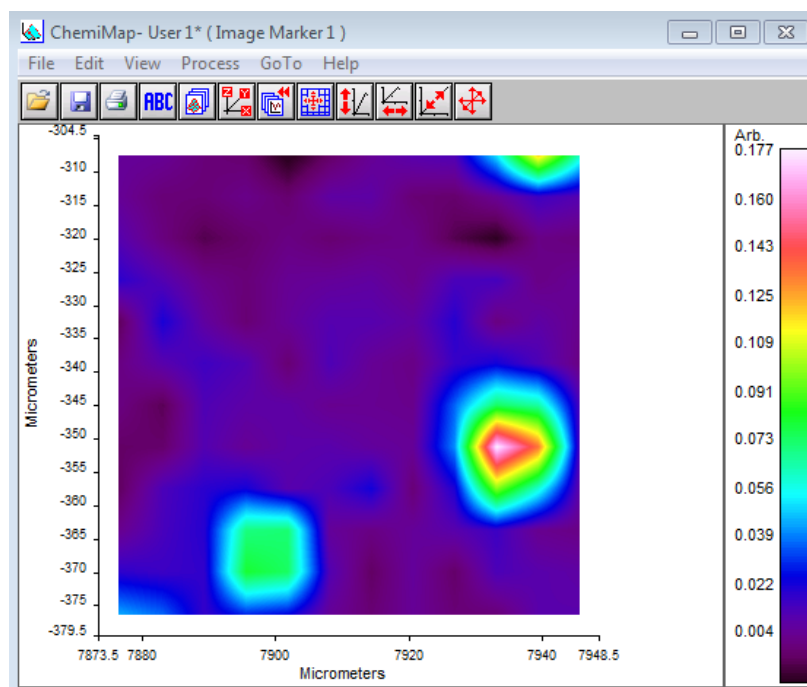


**Figure 3.3:** A 2D contour image of 2 gibbsite particles after Chemimap is used. It is clearly much more obvious that there are two particles in this region, as opposed to the information illustrated from Figure 3.2.

Once the 9 usable particle spectra are found, they are then examined with SPECTRUM software for background cancellations, smoothing, baseline corrections, and other such related refining tools.



## Chapter 4: Results and Discussion (Mie Theory)

In total, there are 9 usable hydrated, and Figure 4.1 shows them overlaid on top of one another before they are averaged.

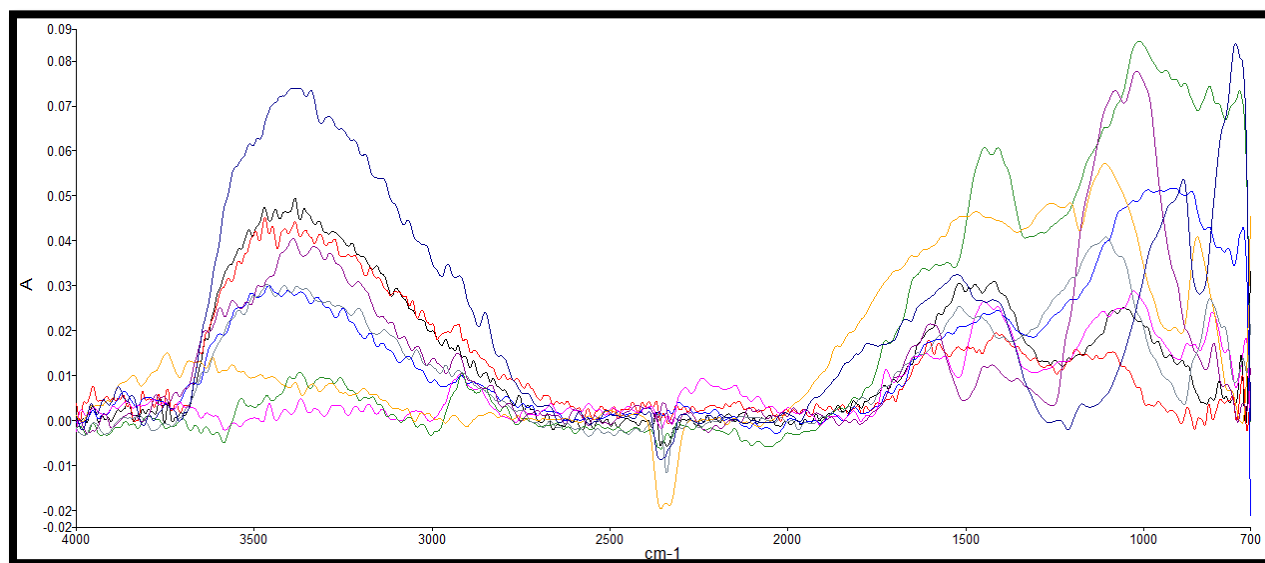


**Figure 4.1:** Nine hydrated alumina spectra, soon to be average for Figure 6.

Although this study is on hydrated alumina, it is worth noting that originally there were thought to be two calibrants: gibbsite and alumina. The results found are interesting because there are  $\text{--OH}$  stretch vibrations of water in the alumina spectra, yet the species is  $\gamma\text{-Al}_2\text{O}_3$ . This odd behavior indicates that the spectra of “alumina” is not actually what is commonly thought to be alumina, but is instead be some form of hydrated alumina:  $\text{Al}_2\text{O}_3 \cdot \text{XH}_2\text{O}$ , where  $X = 0, 1$ , or  $3$ . Furthermore, these  $\text{--OH}$  stretches are not narrow peaks, but are instead broad regions which indicate that the stretches observed are from hydrates. This likely possibility is due to the hydrogen bonding of alumina to water, which produces broad  $\text{--OH}$  stretches. Also, it is understood that there are typically about three monolayers of water are adsorbed on alumina surfaces<sup>11</sup>, and since these particles are micron-sized, there is a lot of surface area exposed to

bind with water. For comparison, Figure 4.2 illustrates a spectrum of what a general, free –OH stretch resembles.

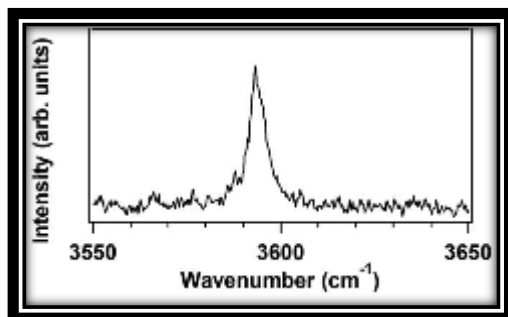


**Figure 4.2:** -OH stretch of pinoresinol using infrared ion-gain spectroscopy (no significant hydrogen bonding)<sup>13</sup>.

The lack of narrow, free –OH stretch vibrations could also be observed when analyzing the results that were supposedly for gibbsite because similar –OH hydrogen stretches are found. In fact, there is really no way to differentiate between the “gibbsite” and “alumina” spectra because they both appeared to form hydrated alumina. Due to this lack of distinction, the spectra data from *both* the gibbsite (2 usable particles) and alumina (7 usable particles) are averaged together (Figure 4.3). Overall, these behaviors help lead to the conclusion that the “two calibrants” are in fact the same chemical.

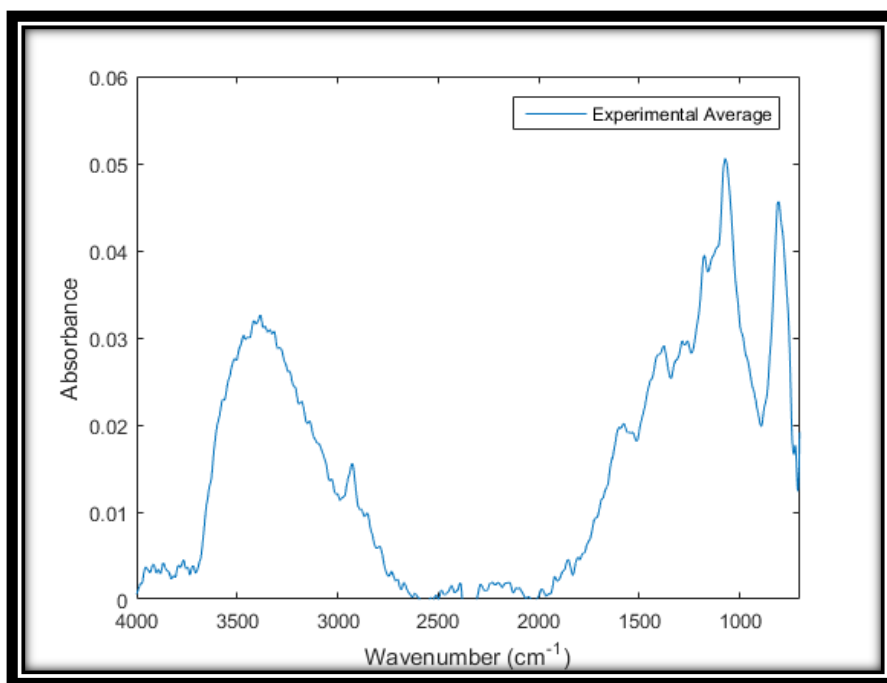


**Figure 4.3:** Average of 9 particle spectra of hydrated alumina

## Chapter 5: Results and Discussion (Mie-Bruggeman Theory)

The result from Mie is a predicted spectra that fits well with the experimental average, seen overlaid in Figure 5.1:

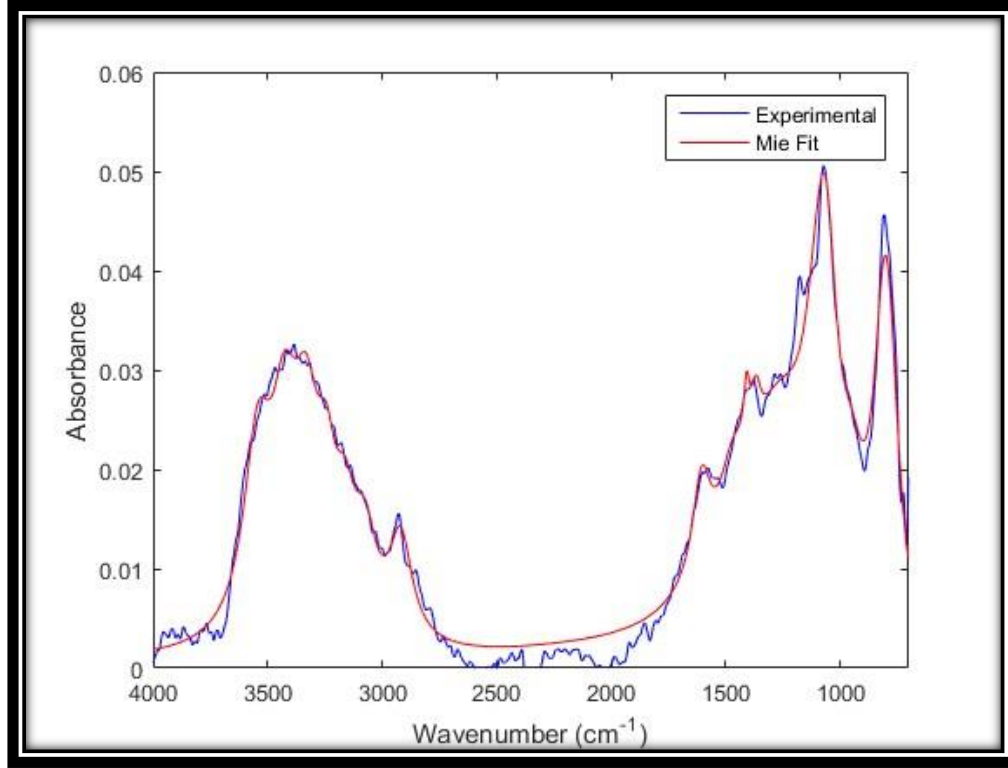


**Figure 5.1:** The average fit from Figures A1-A7 graphed with the experimental fit from Mie Theory. From the Mie fit, one can also obtain the permittivity of this hydrated alumina mixture.

Equation 1 is the equation that gives these parameters (based on Mie theory), and Table 1 shows the parameters used to create the Mie fit spectrum.

$$m^*(\tilde{\nu}) = \sqrt{\varepsilon(\tilde{\nu})} = \sqrt{\varepsilon_0 + \sum_j \frac{A_j \tilde{\nu}_{0,j}^2}{\tilde{\nu}_{0,j}^2 - \tilde{\nu}^2 - i\Gamma_j \tilde{\nu}}} \quad (1)$$

**Table 1:** Hydrated Alumina Mie Fit Parameters of the Average of 18 Particle Spectra; the Fitted Radius is 2.178  $\mu\text{m}$  and  $\epsilon_0 = 1.75$ .

$\nu$ ( $\text{cm}^{-1}$ )	A	$\Gamma$ ( $\text{cm}^{-1}$ )
807	1.45E-02	110.2
779	5.48E-03	99.6
1269	1.34E-02	382.0
765	1.78E-03	118.6
1059	8.22E-03	120.6
949	3.82E-03	130.7
1100	4.98E-03	142.1
1368	3.67E-04	52.9
1408	2.30E-04	30.9
1469	1.20E-03	145.8
1604	9.03E-04	95.9
2920	3.27E-04	123.5
3075	2.60E-04	125.4
3162	2.329E-04	111.5
3243	2.46E-04	104.6
3331	5.34E-04	144.5
3426	4.47E-04	138.7
3543	4.82E-04	151.4

The hydrated alumina can be added as a calibrant for Mie-Bruggeman modeling of dust libraries. An overview of this technique and expected results are given, although this research has not yet gone far enough to test the calibrants studied in this thesis. The idea behind a Mie-Bruggeman spectral model is that one can predict the orientationally-averaged IR spectra of a set of individual, mixed-composition particles<sup>5</sup>. By trapping calibrants in mesh, an average of the individual particle spectra are fit by a Mie theory model and are tabulated as dielectric functions of each component. Mie theory is used to model the spectra of small, homogenous particles comparable in size to the wavelength of light. This model requires calibration in the form of spectra of individual pure particles that are known to be in the particulate matter of interest. One inputs the particle radius ( $r$ ) and complex index of refraction ( $m$ ) (as function of wavenumber),

and the output is a series solution to Maxwell's equations that yield complex Mie coefficients<sup>5</sup>. The index refraction, which is a function of wavenumber, is also the square root of permittivity ( $\varepsilon$ ) (refer to Equation 1 above).

The permittivity of a material requires vibrational information, including  $A_j$ ,  $\tilde{\nu}_{0,j}$ , and  $\Gamma_j$ , which are intensity, position, width, respectively. To obtain these coefficients – as well as the extinction, scattering, and absorption spectrum – a program was written in Fortran using Bohren and Huffman's well-known subroutine. Also note that  $\varepsilon_0$  is the constant, generic part of the complex dielectric function,  $j$  is an index over the vibrations,  $A_j$  is the unit-less strength of the vibrational transition,  $\tilde{\nu}_{0,j}$  is the position of the transition in wavenumber units, and  $\Gamma_j$  is the full-width-at-half-max of the resonance in wavenumber units<sup>5</sup>. Next, the Bruggeman model is run to find an effective dielectric of the mixture based on the pure calibrants. Bruggeman theory, in short, is a simple, effective medium theory that provides an effective permittivity,  $\varepsilon_{eff}$ , of a mixture based on the pure permittivities of the components,  $\varepsilon_i$ , and the component volume fraction,  $f_i$ <sup>(6)</sup>. The model starts with a numerical, iterative approach starting with an initial guess of the volume fractions (Equation 2), which is then used to obtain an initial guess of the effective permittivity. The

$$\begin{array}{lll}
 \text{Bruggeman Theory} & \text{Initial Guess of} & \text{Dielectric Function of} \\
 & \text{Volume Fractions} & \text{Mixture} \\
 \sum_i f_i \frac{\varepsilon_i - 2\varepsilon_{eff}}{\varepsilon_i + 2\varepsilon_{eff}} = 0, & \varepsilon_{eff,0} = \sum_{i=0}^{n-1} f_i \varepsilon_i & \varepsilon_{eff,k} = \frac{\sum_{i=0}^{n-1} \frac{f_i \varepsilon_i}{\varepsilon_i + 2\varepsilon_{i,k-1}}}{\sum_{i=0}^{n-1} \frac{f_i}{\varepsilon_i + 2\varepsilon_{i,k-1}}}
 \end{array} \quad (2)$$

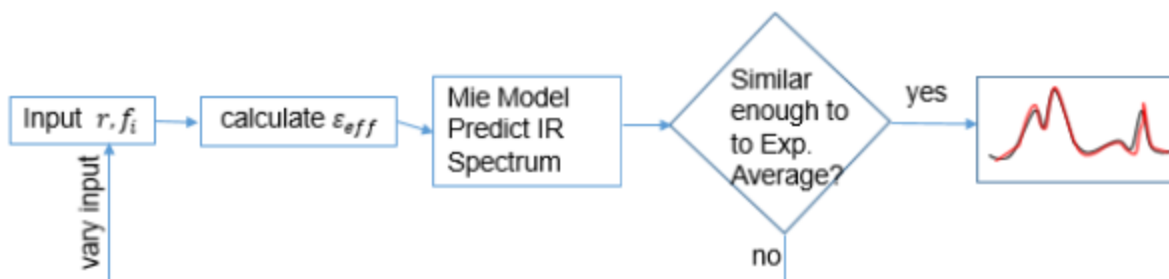


**Figure 5.2:** Flow diagram for a visual representation of Mie-Bruggeman theory<sup>2</sup>.

After, the effective permittivity of the mixture is used with Mie theory to predict an orientationally-averaged IR spectrum of an average particle of the mixed sample<sup>6</sup>. Then, the volume fractions are varied in a nonlinear least squares approach while comparing to the experimental average spectrum in order to find the best fit. Figure 5.3 illustrates the best fits for lab air dust, house dust, and the World Trade Center 9/11/2001 event. Figure 5.4 gives the volume fraction of each calibrant.

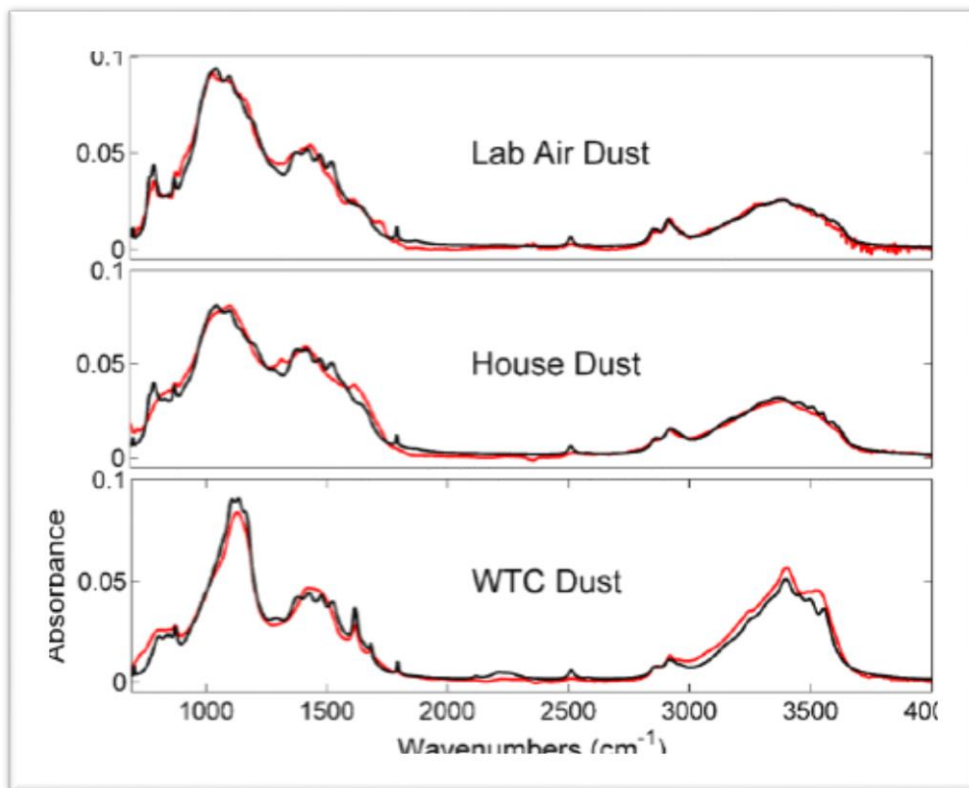


**Figure 5.3:** Mie-Bruggeman model fits. Mixture model fits of the average IR spectra from single particle collections of lab air, house dust from a filter, and the WTC 9/11/2001 event<sup>6</sup>.

Volume Fractions			
Calibrant	Lab Air %	House Dust %	WTC %
quartz	24	15	2
carbonate	12	12	11
clay	24	18	0
gypsum	5	1	50
organics	34	53	36

**Figure 5.4:** Volume fractions for given calibrants, which are iteratively calculated from the Bruggeman theory from the equation presented in Figure 8<sup>6</sup>.

Although these five calibrants have been studied, it is likely that there remain other unknown calibrants present in the dust. For instance, as previously mentioned, there is more elemental Al in dust than what has been accounted for in composition. Gibbsite and alumina are



analyzed because they are both relatively common aluminum-containing compounds, particularly in soils.

## Chapter 6: Future Work and Conclusions

After the Mie-Bruggeman analysis is done for hydrated alumina, it would be wise to check for other calibrants that are both in as well as not yet in the dust library, such as different organics, clays, and carbonates. These compounds can include humic acid salt, polyethylene, kaolinite, montmorillonite, illite, calcite, dolomite, gypsum, and quartz. Kaolinite is a favored weathering product in warm, humid environments<sup>8</sup>. Illite is favored in midlatitude weathering conditions and is also observed in dust collected over the world's oceans. Another attractive reason to study these calibrants is that there are very little regional mineralogical differences<sup>9</sup> (for quartz, there is no difference).

One of the former OSU undergraduates also studied snowpile dust, but since no calibration data have yet been found, one could also incorporate the calibrants for those dust samples. Dust samples from Steubenville, Ohio, are also of interest because they contain unidentified compounds, and the city is relatively close to OSU itself.

Overall, this analysis illustrates how hydrated alumina could lead to the conclusion that this calibrant is part of the dust library, and it is also performed to show that basically any dust can be analyzed in a plasmonic mesh. More specifically, it could provide insight related to health or environmental concerns if, for instance, high levels of hydrated alumina in dust in a particular location is correlated with known medical or environmental risks.

## Bibliography

- <sup>1</sup>Yoshikazu Hashimoto, Yoshika Sekine, *Atmospheric Aluminum from Human Activities*. Atmospheric environment, Vol. 26B, No. 3, pp. 295 – 300, 1992.
- <sup>2</sup>J.V. Coe, D.B. Lioi, L. Shaffer, M.A. Malone, A. Luthra, A. Ravi, *Plasmonic spectra of individual subwavelength particles under the infrared microscope: cells and airborne dust*. Proceedings of SPIE, 8957(Plasmonics in Biology and Medicine XI), 89570A/1-89570A/9 (2014).
- <sup>3</sup>Marvin Malone, Matthew McCormack, J. V. Coe, *Single Airbone Dust Particles using Plasmonic Metal Films with Hole Arrays*. JPCL, 2012, 3, p.g. 720 – 724.
- <sup>4</sup>Marvin Malone, Katherine Cilwa, Antriksh Luthra, Matthew McCormack, David Lioi, J.V. Coe, *Plasmonics Under the Infrared Microscope: Sensing and Spectra of Single Particles Using Metal Film Hole Arrays*. IEEE, 978-1-4577-0911-1/12/\$31.00, 2012.
- <sup>5</sup>David Lioi, Katherine Cilwa, Matthew McCormack, Marvin Malone, J.V. Coe, *Infrared Spectral Model for Subwavelength Particles of Mixed Composition based on the Spectra of Individual Particles with Calibration Data for Airbone Dust*. JPCL, 2013, 117, 11297 – 11307.
- <sup>6</sup>A. Luthra, A Ravi, *The Dust Library: Enhanced Infrared Spectra of Individual Respirable Dust Particles*. International Conference on Environmental Systems. 12-16 July 2015, Bellevue, Washington.
- <sup>7</sup>*Long-range transport of mineral dust in the global atmosphere: Impact of African dust on the environment of the southeastern United States*. Proc. Natl. Acad. Sci. USA. Vol. 96, pp. 3396–3403.
- <sup>8</sup>Pierzynski, G. 2015. *Soils and Environmental Quality*. CRC-Press, 2000. Chapter 2. Prospero, J (1990).
- <sup>9</sup>Huang, Yuncong Li, Malcolm E. Sumnerk. *Handbook of Soil Sciences: Properties and Processes, Second Edition edited by Pan Ming*.
- <sup>10</sup>Grégory Lefèvre et. al. *Hydration of  $\gamma$ -Alumina in Water and Its Effects on Surface Reactivity*. Langmuir. Vol. 18 (2002), pp 7530 – 7537.
- <sup>11</sup>Peter J. Eng et. al. *Structure of the Hydrated  $\alpha$ -Al<sub>2</sub>O<sub>3</sub> (0001) Surface*. Science. Vol 288, 12 May 2000. pp 1029-1033
- <sup>12</sup>Courtney R. Usher et. al. *Reaction on Mineral Dust*. Chem. Rev. 2003, 103, 4883-4939.
- <sup>13</sup>Jacob C. Dean et. al. *Single-conformation UV and IR spectroscopy of model G-type lignin dilignols: The  $\beta$ -O-4 and  $\beta$ - $\beta$  linkages*. Royal Society of Chemistry, 2014, DOI: 10.1039/c3sc53260g.

## **Appendix A: Individual Hydrated Alumina Spectra Sorted by Bottle**

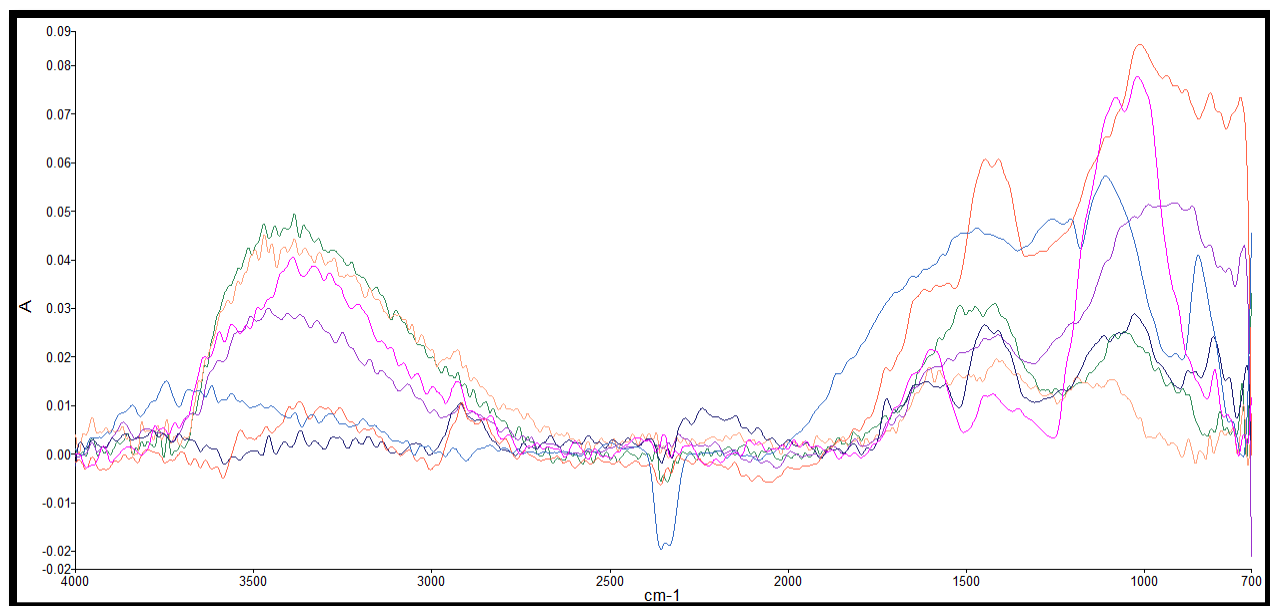


**Figure A1:** Individual hydrated alumina particles from bottle labeled "alumina."

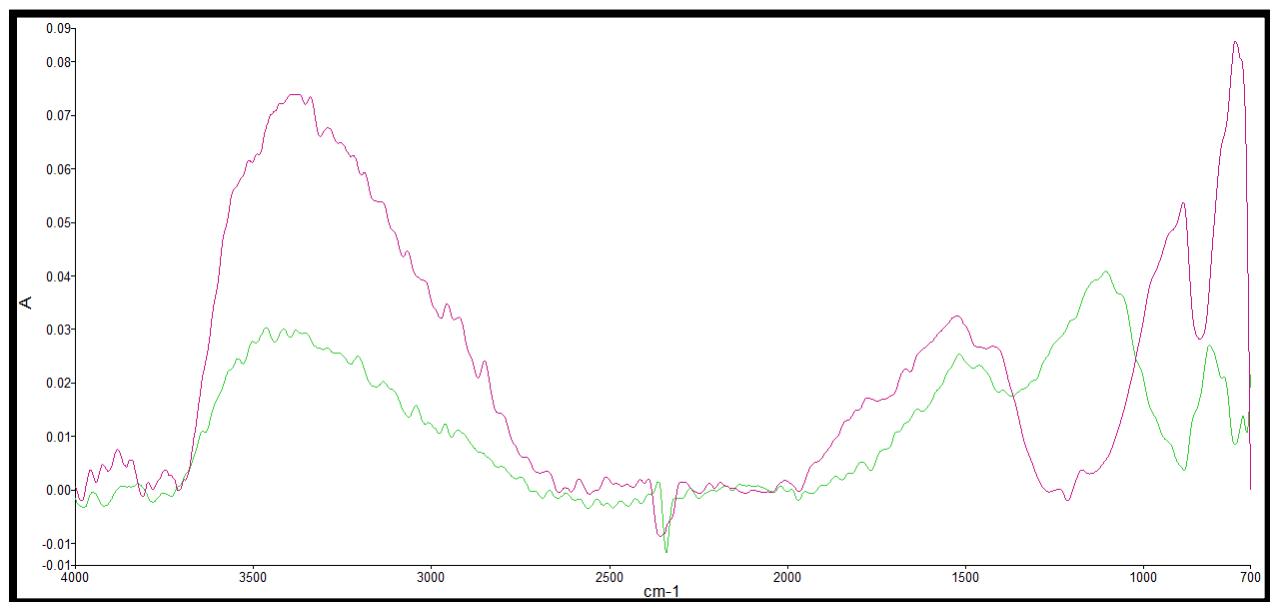


**Figure A2:** Individual hydrated alumina particles from bottle labeled "gibbsite."